Photochemistry and Photobiology, 2007, 83: 1254–1262

Light-Driven Horseradish Peroxidase Cycle by Using Photo-activated Methylene Blue as the Reducing Agent

Vanessa A. Soares[1], Divinomar Severino[2], Helena C. Junqueira[2], Ivarne L. S. Tersariol[1], Cláudio S. Shida[1], Maurício S. Baptista[2], Otaciro R. Nascimento[3] and Iseli L. Nantes*[1]

[1]Centro Interdisciplinar de Investigação Bioquímica, Universidade de Mogi das Cruzes, Mogi das Cruzes, SP, Brazil
[2]Depto de Bioquímica, Instituto de Química, Universidade de São Paulo, São Paulo, SP, Brazil
[3]Instituto de Física, Universidade de São Paulo, São Carlos, SP, Brazil

Received 29 December 2006; accepted 26 April 2007; DOI: 10.1111/j.1751-1097.2007.00158.x

ABSTRACT

In this work, the regeneration of native horseradish peroxidase (HRP), following the consecutive reduction of oxo-ferryl π-cation (compound I) and oxo-ferryl (compound II) forms, was observed by UV–visible spectrometry and electron paramagnetic resonance (EPR) in the presence of methylene (MB^+), in the dark and under irradiation. In the dark, MB^+ did not affect the rate of HRP compound I and II reduction, compatible with hydrogen peroxide as the solely reducing species. Under irradiation, the dye promoted a significant increase in the native HRP regeneration rate in a pH-dependent manner. Flash photolysis measurements revealed significant redshift of the MB^+ triplet absorbance spectrum in the presence of native HRP. This result is compatible with the dye binding on the enzyme structure leading to the increase in the photogenerated $MB^{\cdot}$ yield. In the presence of HRP compound II, the lifetime of the dye at 520 nm decreased ~75% relative to the presence of native HRP that suggests $MB^{\cdot}$ as the heme iron photochemical reducing agent. In argon and in air-saturated media, photoactivated MB^+ led to native HRP regeneration in a time- and concentration-dependent manner. The apparent rate constant for photoactivated MB^+-promoted native HRP regeneration, in argon and in air-saturated medium and measured as a function of MB^+ concentration, exhibited saturation that is suggestive of dye binding on the HRP structure. The dissociation constant (K_{MB}) observed for the binding of dye to HRP was 5.4 ± 0.6 μM and 0.57 ± 0.05 μM in argon and air-saturated media, respectively. In argon-saturated medium, the rate of the conversion of HRP compound II to native HRP was significantly higher, $k_{2argon} = (2.1 \pm 0.1) \times 10^{-2} s^{-1}$, than that obtained in air-equilibrated medium, $k_{2air} = (0.73 \pm 0.02) \times 10^{-2} s^{-1}$. Under these conditions the efficiency of photoactivated MB^+-promoted native HRP regeneration was determined in argon and air-equilibrated media as being, respectively: $k_2/K_{MB} = 3.9 \times 10^3$ and 12.8×10^3 $M^{-1} s^{-1}$.

INTRODUCTION

Horseradish peroxidase (HRP) is a heme containing enzyme catalyzing the oxidation by hydrogen peroxide of a wide variety of inorganic and organic compounds such as iodide, bromide, ascorbate, ferrocyanide, cytochrome *c* and the leuco form of many dyes (1). The term HRP is used somewhat generically as the root of horseradish (*Armoracia rusticana*) contains a number of distinctive peroxidase isoenzymes of which the C isoenzyme (HRP C) is the most abundant (1). HRP C comprises a single polypeptide chain with 308 amino acid residues. The enzyme structure exhibits four disulfide bridges between cysteine residues 11–91, 44–49, 97–301 and 107–209, and a buried salt bridge between Asp99 and Arg123. Sites of glycosylation are in loop regions of the structure at Asn13, Asn57, Asn158, Asn186, Asn198, Asn214, Asn255 and Asn268, and bear branched heptasaccharides that account for 75–80% of the glycans. These oligosaccharides invariably contain two terminal GlcNAc and several mannose residues (2,3). The enzyme structure exhibits two Ca^{2+} ions: one of them is coordinated with Asp43, Asp50, Ser52 (side chains) and Asp43, Val46, Gly48 (carbonyl groups) and a structural water, and the other one is coordinated with Thr171, Asp222, Thr225, Asp230 (side chains) and Thr171, Thr225 and Ile228 (carbonyl groups). The heme group exhibits the heme iron pentacoordinated bearing His170 as the distal ligand (4). Five oxidation states of HRP, ferrous, ferric, compounds I and II, oxy-ferrous, are known and formed during the peroxidase and oxidase cycles of the enzyme. In the peroxidase cycle the Fe(III) heme iron of the resting enzyme coordinates a deprotonated hydrogen peroxide molecule to form compound 0. In this step, recent literature data suggest that His42 acts initially as a proton acceptor (base catalyst) and then as a donor (acid catalyst) at neutral pH, consistent with the observed slower rate and lower efficiency of heterolytic cleavage observed at acid pH. Arg38 is influential in lowering the p*K*a of His42, as well as in aligning HOOH in the active site, but it does not play a direct role in proton transfer. Compound 0 is turned into compound I (oxoferryl π-cation radical) by the heterolytic cleavage of HOOH and generates the reduced form of the peroxide (water for HOOH and alcohol-derived for ROOH). Compound I is converted to compound II (oxoferryl heme iron) by attacking another peroxide molecule or another reducing agent as depicted by Scheme 1. Compound II returns to the native form by attacking

*Corresponding author email: ilnantes@umc.br (Iseli L. Nantes)

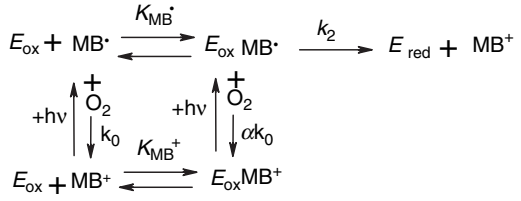

Scheme 1. Routes for electron transfer from $MB^{\bullet}$ to HRP in the presence and in the absence of O_2.

another molecule of the reducing agent. In the oxidase cycle the ferric enzyme can be reduced to the ferrous form and, in the presence of molecular oxygen, converted to compound III. The electronic structure of compound III of HRP is similar to that of oxymyoblogin and oxyhemoglobin and can be described as Fe^{2+}-O_2 or the isoelectronic Fe^{3+}-O_2^-. The dioxygen bound to HRP has a significant superoxide character and is highly reactive. Compound III can also be generated by the reaction of compound II with excess of peroxide and can return to the native form by the detachment of the superoxide ion (1,5,6).

As cited above, HRP can use a wide variety of reducing agents to reduce the high valence intermediates. Literature data describe that a parent enzyme produced by the fungus *Phanerochaete chrysosporium*, the lignine peroxidase (Lip), can oxidize various heterocyclic dyes including methylene blue (MB^+) (7–9). In this regard, MB^+ exhibits photochemical properties and it is a sensitizer used *in vitro* for a variety of applications, including energy conversion and photodynamic therapy (10). The photoexcitation of MB^+ leads the dye to the triplet excited state *via* intersystem crossing. In the monomer form, predominant at low concentrations (up to 8 μM) or in the presence of excess of SDS, MB^+ generates singlet oxygen ($O_2(^1\Delta g)$) (Type II mechanism) *via* energy transfer to ground state molecular oxygen. At high concentrations, triplet MB^+, aggregated as dimer, generates dye-derivate free radicals $MB^{2+\bullet}$ and $MB^{\bullet}$ (Type I mechanism) (11). The neutral radical of the dye, $MB^{\bullet}$, is a reducing agent able to reduce ferric cytochrome *c* (12). For peroxidases, literature data have shown the use of the chemical and electrochemical reducing potential of MB^+ to reduce the oxidized intermediates of the enzymes (13,14). However, the photogenerated $MB^{\bullet}$ is also a potential reducing agent for the peroxidases. Investigation concerning peroxidase reactions in the presence of photoexcited MB^+ was reported for the peroxidase-oxidase (PO) oscillator (15). In this model for complex reaction network, where NADPH is the principal electron donor (14,16–18) the interference in the oscillations were interpreted as coming from the excited MB^+-promoted NADPH oxidation. In this work, for the first time, a light-driven catalytic cycle of HRP with the intermediacy of photoexcited MB^+ is described. This finding brings to light the potential use of this system in nanotechnology and energy transduction.

MATERIALS AND METHODS

Chemicals. Horseradish peroxidase (Type VI–A) was obtained from Sigma Chemical Co. (St. Louis, MO). Hydrogen peroxide and MB^+ were purchased from Aldrich (Milwaukee, WI). The concentration of the dilute HOOH solutions and HRP solutions were always checked spectrophotometrically using the molar extinction coefficient at 240 nm (HOOH), $\epsilon_{240} = (39.4 \pm 0.2)\,\text{M}^{-1}\,\text{cm}^{-1}$ and 403 nm (HRP), $\epsilon_{403} = 1.02 \times 10^5\,\text{M}^{-1}\,\text{cm}^{-1}$ (19). All aqueous solutions were prepared with deionized water (mixed bed of ion exchanger, Millipore) and the pH was measured using a combined glass electrode (Orion Glass pH SURE-FLOW). The reference electrode (ROSS, Model 8102) was filled with Orion Filling Solution (ROSS). The pH meter was calibrated using METREPAK pHydrion standard buffer solutions (Brooklyn, NY).

Irradiation system. Samples in 5 mM phosphate buffer, at 25°C, were irradiated in a glass chamber with a halogen light bulb of 500 W power, set at a distance of 30 cm. Irradiance was measured with calibrated detectors and a meter (Fieldmate-Coherente). In this condition, the power reaching the sample was measured by the power meter as being ~10 mW. The glass chamber was cooled by circulating water.

UV–Vis measurements. All spectra were performed in a Photodiode Array Spectrophotometer MultiSpec-1501 (Shimadzu Co., Kyoto, Japan).

Enzymatic kinetics. The data sets represent the average of three independent measurements. The kinetic data were recorded at 403 nm, the Soret band wavelength peak of the HRP native. The observed conversion of HRP compound II into HRP native obeys a relationship that could be fit to the first-order (Eq. 1).

$$\Delta A_{403\text{nm}} = \text{lim} \times \left(1 - e^{(-k_{\text{obs}} \times t)}\right) \quad (1)$$

where $\Delta A_{403\text{nm}}$ and *lim* are the concentration of native HRP regenerated at a given time and at infinite time, respectively, and k_{obs} is the observed first-order rate constant for the conversion of HRP compound II to the native form.

The influence of dye concentration on the conversion rate of HRP compound II to the native form obeyed (Eq. 2):

$$k_{\text{obs}} = \frac{k_{\text{obs}_{\text{max}}} \times [\text{MB}]}{k_{\text{MB}} + [\text{MB}]} \quad (2)$$

where k_{obs} is the observed conversion rate of HRP compound II to the native form, k_{obsmax} is the maximum rate, [MB] is the concentration of the dye, and K_{MB} is the apparent dynamic or pseudoequilibrium constant for complexation between HRP compound II and the dye.

The influence of pH on the conversion rate of HRP compound II to the native form by hydrogen peroxide obeyed (Eq. 3):

$$k_{\text{obs}} = \frac{\text{lim} \times 10^{\text{pH}-\text{p}K_a}}{10^{\text{pH}-\text{p}K_a} + 1} \quad (3)$$

where *lim* = k_{obs} independent of pH and k_{obs} is the observed first-order rate constant for the conversion of HRP compound II to the native form.

Laser flash photolysis. The data were obtained with an Applied Photophysics system composed of a Nd:YAG laser (Spectron Laser System, Warwickshire, UK), operating at 532 nm, delivering pulses with 30 mJ/pulse and 10 ns (full width at half maximum), and a pulsed 150 W Xe lamp. Control electronics and a Hewlett–Packard model 54510B digitizing oscilloscope interfaced to a PC were used for data capture.

EPR spectrometry. Direct EPR measurements of heme iron signal were obtained in a Bruker ELEXSYS EPR System E-580, X-band spectrometer under the following conditions: gain 45 dB, modulation amplitude 1.0 mT, microwave power 0.64 mW, microwave frequency 9.47 GHz, center magnetic field 240.0 mT, scan range of magnetic field 410.0 mT, temperature variation between 4 and 50 K, time constant 10.24 ms and conversion time 40.96 ms. After mixing, solutions were quickly introduced into an EPR quartz tube that was previously cooled in liquid nitrogen. After freezing, the sample was introduced into the microwave cavity at low temperature and the EPR measurements were performed.

Docking simulations. Docking simulations with flexible ligand were performed by using ArgusLab software (20). The HRP template was 1H55 from Protein Data Bank. The ligand molecules were MB^+ and the corresponding neutral form.

RESULTS

Figure 1a shows the changes in the HRP and MB^+ spectra in the presence of hydrogen peroxide and under irradiation. The thick solid line represents the spectrum of HRP in the presence of MB^+ before the addition of hydrogen peroxide. The HRP spectrum, in the presence of MB^+, remains unchanged in the absence of hydrogen peroxide both in the dark and under irradiation (data not shown). The addition of hydrogen peroxide leads to changes in the HRP spectrum compatible with the formation of compound II (dotted line) as the Soret band was shifted from 403 to 418 nm. In this condition, the Q bands of HRP spectrum were also compatible with the formation of compound II but they were overlapped by the MB^+ spectrum. The irradiation of the sample with a 500 W halogen lamp led to the rapid return of HRP compound II to the native form (k_{obs} = 0.395 min^{-1}). Figure 1b shows the spectra of HRP and MB^+ during the reaction with hydrogen peroxide in the dark. In the ground state, MB^+ did not affect the rate of HRP compound II spontaneous decay (k_{obs} = 0.066 min^{-1}) compatible with hydrogen peroxide as the solely reducing species. In the course of the reaction carried out under irradiation (Fig. 1a), MB^+ exhibits 5 nm blueshift of the visible band peaking at 665 nm. The ratio of the visible band peak intensity/absorbance intensity at 620 nm was also changed from 1.81 to 1.56. These MB^+ spectral changes were not observed during the HRP catalytic cycle in the dark (Fig. 1b) and under irradiation in the absence of hydrogen peroxide (data not shown). This result suggests that aggregated forms of the dye should be consumed in the reaction. The blueshift exhibited by the MB^+ visible band peak (Fig. 1a) could be assigned to the formation of photoproducts from the oxidized form of the dye or from the reaction of MB· and MB^{2+} with the protein structure to form protein adducts as has been observed with other positively charged dyes (21).

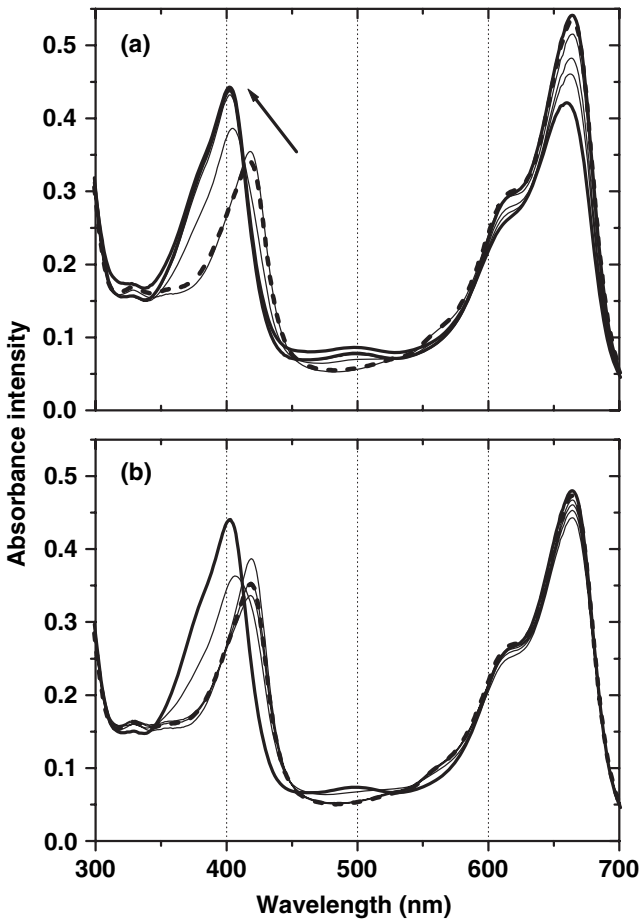

Figure 1. UV–visible spectra of HRP in the course of the reaction with hydrogen peroxide. (a) In the presence of MB^+ under irradiation before (thick solid line) and 15 s after the addition of hydrogen peroxide (dotted line). The thin solid lines represent, according to the arrow, the spectra obtained at 1, 5, 10 and 20 min after the addition of hydrogen peroxide. (b) In the presence of MB^+ in the dark at time 0 (thick solid line) and 15 s after the addition of hydrogen peroxide (dotted line). The thin solid lines represent, according to the arrow, the spectra obtained at 1, 5, 10 and 20 min after the addition of hydrogen peroxide. The reaction was carried out in 5 mM phosphate buffer, pH 8.0, at 30°C. The hydrogen peroxide and HRP concentrations were 6 and 4 μM, respectively.

These results indicate that the excited state of MB^+ is involved in the reduction of the high valence intermediates of HRP, compounds I and II. The participation of the excited state of MB^+ in the completion of HRP cycle also became evident when the pH curves for the reduction of compound II in the presence and in the absence of photoactivated MB^+ are compared (Fig. 2).

In Fig. 2, the pH curve for the HRP cycle in which hydrogen peroxide was used as both oxidant and reducing agents reveals, as expected for HRP C (22), that the reaction exhibited a pH curve with pK_a around 8.5 (black solid circles). In the presence of photo-activated MB^+ (gray solid circles), the pH curve for the HRP cycle revealed increase in the reaction rate over all the investigated pH range. In this condition, the maximal rate is attained at pH 7.0. The subtraction of the pH curve obtained in the absence of photo-activated MB^+ (black solid circles) from the pH curve obtained in the presence of photo-activated MB^+ (gray solid circles) resulted in a pH curve with one transition at pH ~6.25 (gray solid triangles). The pK_a ~6.25 matched with that determined for the triplet MB^+ k_{obs} (black solid triangles). These results are in accord with the neutral radical $MB^•$ as the reducing agent for the HRP high valence intermediates. The possibility that the superoxide ion generated by electron transfer from $MB^•$ to molecular oxygen was the reducing agent has been excluded as the presence of molecular oxygen disfavored significantly the reaction (Fig. 3a–c).

At this point it was important to investigate the effect of both MB^+ concentration and the presence of oxygen on the rate of HRP compound II reduction (Fig. 3a–c). Figure 3a,b, illustrates a representative time course of native HRP regeneration by photoactivated MB^+ in argon- and in air-saturated media, respectively. It can be observed that, in both conditions, photoactivated MB^+ led to native HRP regeneration in a time- and concentration-dependent manner. The apparent rate constant for photoactivated MB^+-promoted native HRP regeneration, in argon- and in air-saturated medium, was measured as a function of MB^+ concentration to determine the second-order constant of the dye (Fig. 3c, closed and open circles, respectively). In both conditions the curve for the rate of the reaction as a function of MB^+ concentration exhibits saturation that is suggestive of dye binding on the HRP

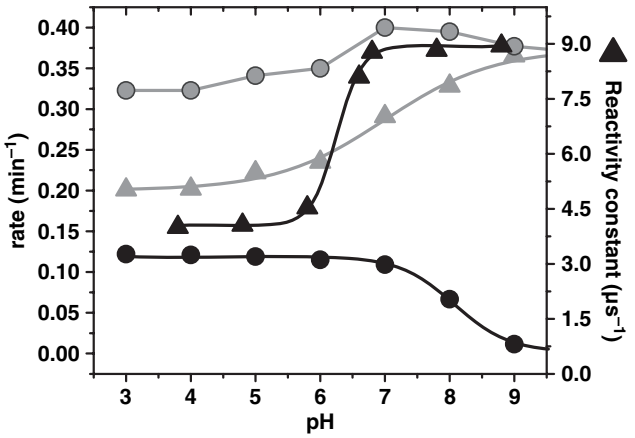

Figure 2. pH profile of the initial rate of native HRP regeneration from compound II and pH profile of triplet MB^+ reactivity. Solid black circles represent the pH profile of spontaneous HRP compound II decay (pK_{aobs} = 8.3); solid light gray circles represent the decay of HRP compound II in the presence of MB^+ and under irradiation; solid light gray triangles represent the subtraction of the pH curve obtained in the presence of MB^+ under irradiation and the pH profile of the spontaneous decay of HRP compound II. The solid black triangles represent the pH profile of triplet MB^+ reactivity obtained as the inverse of triplet MB^+ lifetime (1/lifetime) at different pH values. The reactions were carried out in 5 mM acetate (pH range 3.0–5.0), phosphate (pH = 3.0, pH range 6.0–7.0 and 11.0–13.0) and ammonium hydroxide (pH range 8.0–10.0), at 30°C. The hydrogen peroxide and HRP concentrations were 6 and 4 μM, respectively.

structure. Scheme 1 depicts the model of interaction between HRP and the dye; the dissociation constant (K_{MB}) observed for the binding of dye to HRP was (5.4 ± 0.6) μM and (0.57 ± 0.05) μM in argon- and air-saturated media, respectively. In argon-saturated medium, the rate of conversion of HRP compound II to native HRP was significantly higher, $k_{2argon} = (2.1 \pm 0.1) \times 10^{-2}$ s^{-1}, than that obtained in air-equilibrated medium, $k_{2air} = (0.73 \pm 0.02) \times 10^{-2}$ s^{-1}. This result is coherent, as molecular oxygen is a well-known quencher for triplet species that, in this reaction, could be the precursor of the reducing species for the enzyme. Molecular oxygen can also oxidize $MB^\bullet$ and prevent the electron transfer from the dye to the enzyme. However, it is important to note that the argon purgation in the medium cannot promote complete molecular oxygen depletion and the k_{2argon} value obtained is yet apparent. Under these conditions the efficiency of photoactivated MB^+-promoted native HRP regeneration was determined in argon- and air-equilibrated media, respectively: $k_2/K_{MB} = 3.9 \times 10^3$ and 12.8×10^3 M^{-1} s^{-1}. The higher catalytic efficiency observed in air-equilibrated medium comes from the significantly higher affinity to HRP exhibited by the dye in this condition (K_{MB} ~10-fold lower). Considering Scheme 1, the presence of molecular oxygen is expected to increase the steady state ratio $[MB^+]/[MB^\bullet]$ *via* quencher of the triplet state of the dye and/or the oxidation of its neutral radical. The hydrophobicity of MB^+ could provide affinity to the heme crevice reinforced by the interaction with a negatively amino acid side chain at this site. The loss of the positive charge after the conversion of MB^+ to the reduced form ($MB^\bullet$) could decrease the affinity to the enzyme and at the same time could favor the electron transfer to oxoferryl heme iron.

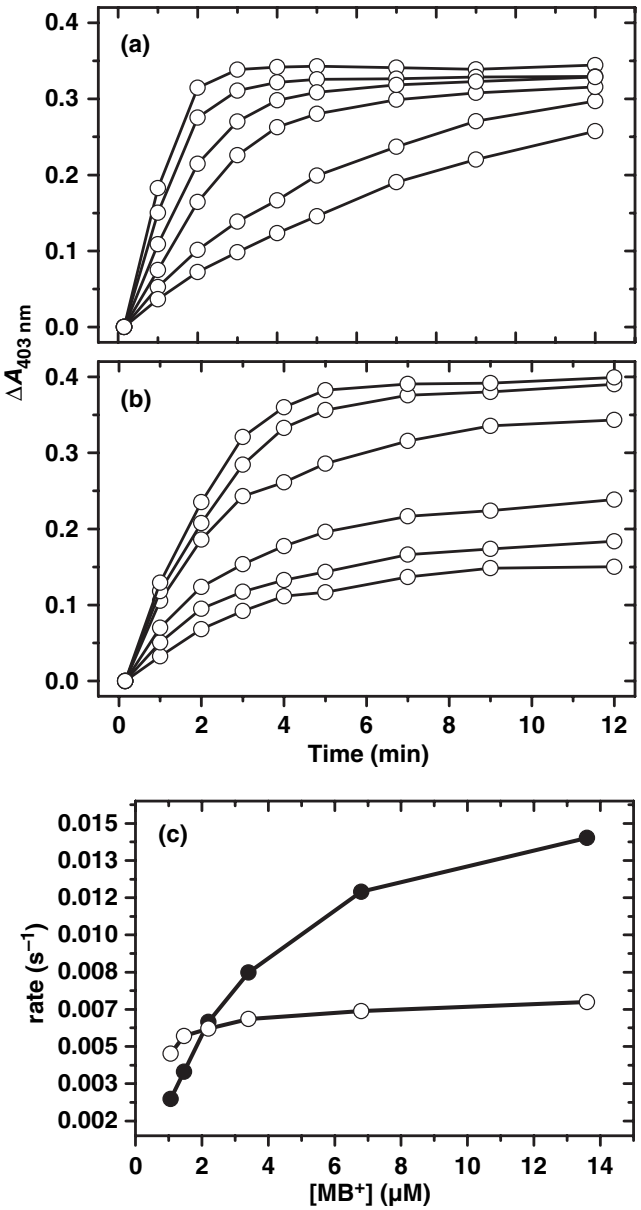

Figure 3. Effect of MB^+ concentration and molecular oxygen on the rate of the decay of HRP compound II. (a) Kinetic of native HRP regeneration in the presence of 1.05, 1.5, 2.2, 3.4, 6.8 and 13.6 μM MB^+ in the dark. (b) The same experiment carried out under irradiation. (c) Curve for the rate of native HRP regeneration as a function of MB^+ concentration. The solid circles represent the results obtained in argon-saturated medium and the open circles represent the results obtained in air-saturated medium. In the argon-saturated medium, the k_2 obtained from (Eq. 1) were: $k_{2argon} = (2.1 \pm 0.1) \times 10^{-2}$ s^{-1}, and $k_{2air} = (0.73 \pm 0.02) \times 10^{-2}$ s^{-1}. The experiments were carried out in 5 mM phosphate buffer, pH 8.0, in the presence of 4 μM HRP, 6 μM hydrogen peroxide, at 30°C.

These results also exclude superoxide ion as the reducing agent for the high valence forms of HRP. There are two possibilities for the photogeneration of $MB^\bullet$ able to reduce HRP high valence intermediates: (1) electron abstraction of another MB^+ molecule bound at the neighborhood (23); (2) electron abstraction of an amino acid side chain of the protein.

The flash photolysis analysis of the reaction contributed to elucidate the reducing MB^+ species responsible for the

reduction of HRP high valence species. Figure 4a,b shows the spectra of 15 μM excited MB^+ in the absence of HRP (opened circles) and in the presence of 15 μM native HRP (black solid circles) obtained at 5 and 10 μs after the laser pulse (Fig. 4a,b, respectively). In both figures, it is clear that the presence of HRP changes significantly the MB^+ triplet spectrum. HRP decreases the contribution of the MB^+ triplet signal (400–420 nm region) and favors the contribution of the $MB^{\bullet}$ signal (430–525 nm region) in the spectra obtained immediately after the MB^+ excitation by the laser pulse (11).

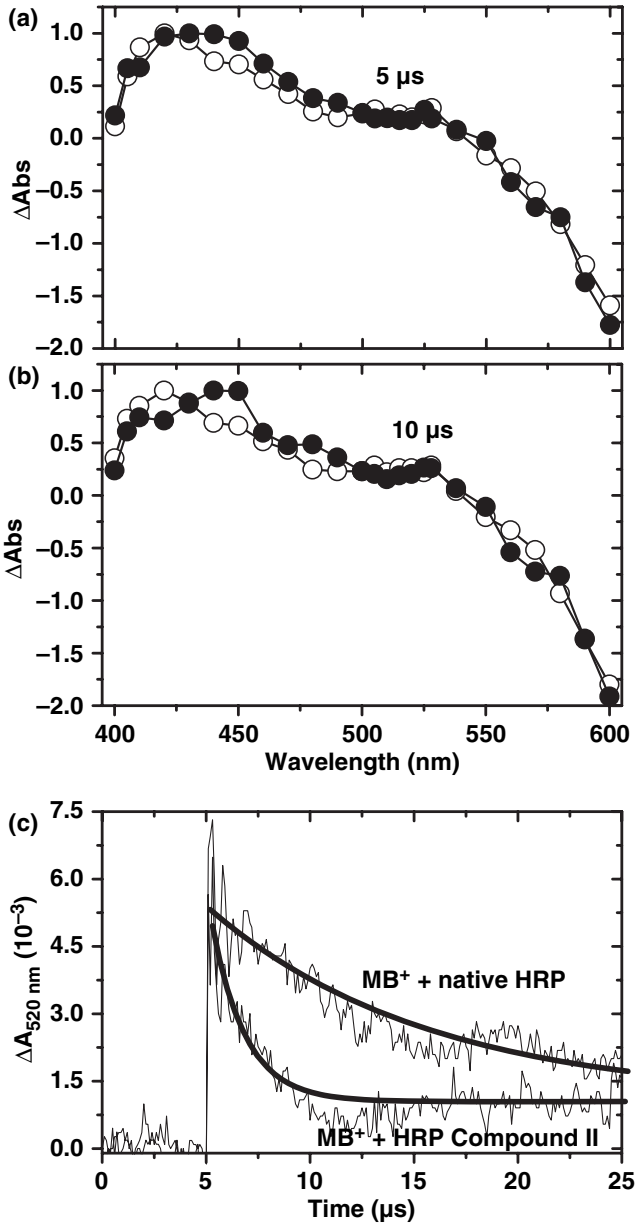

Figure 4. Flash photolysis transient normalized ΔA spectra of MB^+ free and associated with HRP, and effect of HRP on the $MB^{\cdot}$ lifetime. (a) The 15 μM MB^+ triplet spectra obtained 5.0 μs after the laser pulse in the absence of HRP (open circles) and at the same time in the presence of 5.0 μM HRP (solid black circles). (b) The 15 μM MB^+ triplet spectra obtained 10.0 μs after the laser pulse in the absence of HRP (open circles) and at the same time in the presence of 5.0 μM HRP (solid black circles). The experiments were carried out in 5 mM phosphate buffer, pH 8.0, at room temperature. (c) Decay of $MB^{\cdot}$ signal in the presence of native HRP and in the presence of HRP compound II produced by the addition of hydrogen peroxide.

This result suggests that the binding of MB^+ molecules on the HRP structure favors the decay of triplet MB^+ *via* electron abstraction. In this case triplet MB^+ bound in the enzyme structure could abstract one electron from another MB^+ molecule bound closed to the dye excited molecule or the excited MB^+ could abstract one electron from an HRP amino acid residue.

The lifetime of triplet MB^+, measured at 420 nm, was around 10 μs in the absence of HRP and 7 μs in the presence of HRP (data not shown).

Figure 4c shows the decay of $MB^{\bullet}$ signal in the presence of native HRP and in the presence of HRP compounds I and II produced by the addition of hydrogen peroxide in the medium. The lifetime of $MB^{\bullet}$ was 7.5 μs in the absence of HRP (data not shown) and in the presence of 15 μM native HRP, but the conversion of HRP to the high valence form compound II decreased the lifetime of $MB^{\bullet}$ to 2.0 μs. This result corroborates that photochemically-generated $MB^{\bullet}$ is the reducing agent for the high valence forms of HRP.

In order to detect and characterize any radical species formed, the reaction of HRP with H_2O_2 was accompanied by EPR spectroscopy with samples frozen at defined times and run at the indicated temperature. The EPR spectrum of native HRP obtained in 10 mM phosphate buffer, pH 8.0, reveals, at the low field region, the presence of two high spin species of the Fe(III) heme iron ($g = 6.0$) with a quasi-axial symmetry. The proportion between the HRP species could be modulated by varying the ionic strength (data not shown) and the presented condition was chosen to reproduce the conditions used for kinetic experiments. The addition of hydrogen peroxide led to the disappearance of the $g = 6.0$ signal indicating that both HRP conformations were converted to the high valence intermediates. At the same time, the appearance of a relatively broad EPR signal at the high field region ($g = 1.998$) could be observed, characteristic of compound I, oxyferryl porphyrin π-cation radical with antiferromagnetic coupling between the electrons of the heme iron and the porphyrin ring as described by Schulz *et al.* (24) (Fig. 5a). As indicated in Fig. 5a, in the course of the reaction, the HRP heme iron $g = 6.0$ signal was progressively recovered concomitant with the $g = 1.998$ signal disappearance. However, the recovered HRP heme iron signal reveals different proportions of the enzyme species at the end of the catalytic cycle. This spectral change could result from the oxidation of HRP amino acid residues by the high valence forms of heme iron. Before the addition of hydrogen peroxide, the presence of MB^+ slightly altered the HRP EPR spectrum suggesting the selection of a local symmetry of the heme iron. This result is compatible with the binding of MB^+ molecules close to the heme group (Fig. 5b). Figure 5c shows the EPR spectra of HRP in the course of the reaction with hydrogen peroxide, in the presence of MB^+ and under irradiation with a 500 W halogen lamp. Under irradiation, the addition of hydrogen peroxide led to the disappearance of the $g = 6.0$ signal concomitant with the appearance of the $g = 1.998$ signal; however, the catalytic cycle was extremely faster in this condition (240 min in the dark and in the absence of MB^+ and 11 min under irradiation in the presence of MB^+). Figure 5d shows the effect of temperature on the HRP $g = 1.998$ signal. The EPR spectra shown in Fig. 5d were obtained at 4, 8, 10,

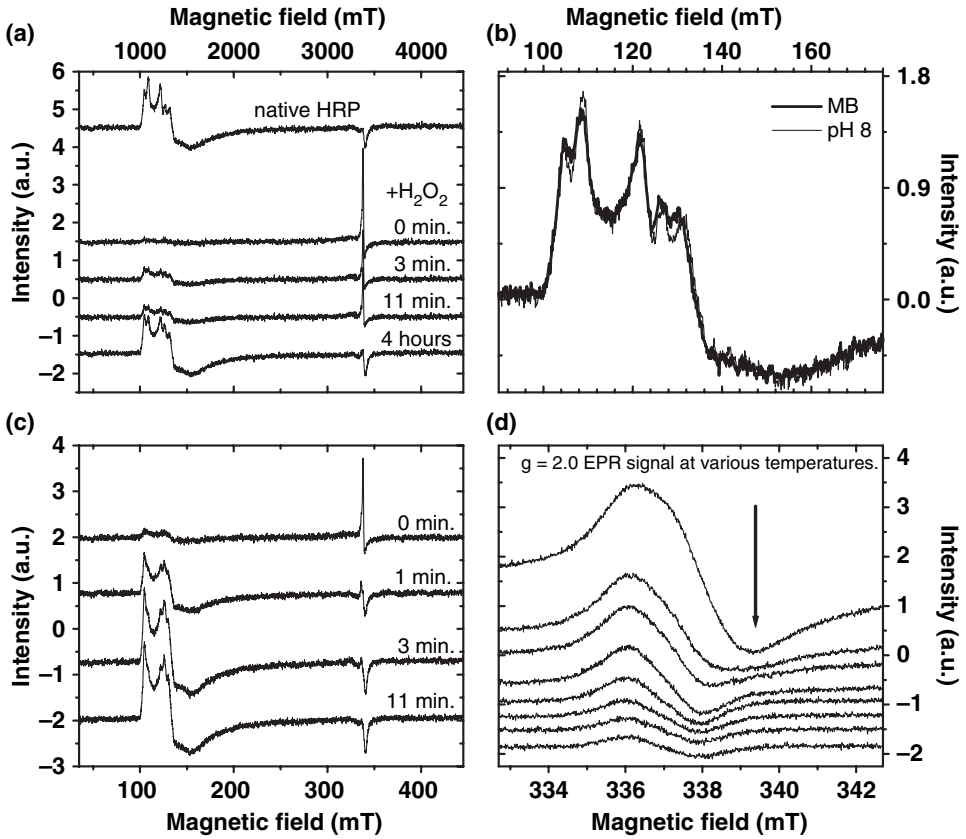

Figure 5. EPR analysis of 100 μM HRP obtained at 11 K in 5 mM phosphate buffer, pH 8.0, in the course of the reaction with hydrogen peroxide. (a) HRP EPR spectra obtained before and 15 s, 3 min, 11 min and 4 h after the addition of hydrogen peroxide. (b) EPR spectra of native HRP in the absence (thin solid line) and in the presence of 100 μM MB^+, before irradiation (thick solid line). (c) HRP EPR spectra obtained at 15 s, 3 and 11 min after the addition of hydrogen peroxide in the presence of MB^+. (d) Effect of temperature on the high field region spectrum. The temperatures were: 4, 8, 10, 13, 20, 30, 40 and 50 K as indicated by the arrow. Frequency of the microwave = 9.47362 GHz, scanning of the magnetic field = 10.0 mT, modulation field = 0. 1 mT, microwave power = 0.64 mW.

13, 20, 30, 40 and 50 K (as indicated by the arrow). The decrease in the $g = 1.998$ signal with the increase in temperature corroborates that this paramagnetic species is not a free radical small molecule. For free radical small molecules, an increase in the EPR signal concomitant with an increase in the temperature at a constant microwave power (0.64 mW, in the conditions of the present work) is expected, as this signal, as a consequence of microwave saturation, is drastically decreased at low temperatures.

Numerical integration of this signal was compatible with the broad signal described in Schulz *et al.* (24) assigned as HRP compound I. Area calculation of the $g = 1.998$ EPR signal showed that this signal corresponds to around 6% of the native HRP EPR signal area. Considering that the EPR experiments were not carried out by using a stopped-flow artifact, the EPR signal detected immediately after hydrogen peroxide addition was from remaining compound I and the missing of the signal means that compound I was almost converted to compound II as attested by the corresponding UV–visible spectrum carried out at the same time interval (Fig. 1a, dotted line).

Considering that the kinetic data, flash photolysis and EPR results strongly supported the binding of MB^+ on HRP, a molecular model for the MB^+ binding in HRP could provide a sketch of the dye/enzyme complex compatible with the experimental results. Figure 6 shows that MB^+ molecules could bind to HRP region at the heme crevice. The molecular model points out the existence of two potential sites for MB^+ binding at the immediacy of the heme group but kinetic data show that the binding of one MB^+ molecule is enough to reduce HRP compound II. Thus, the HRP-bound triplet MB^+ could abstract one electron from an amino acid side chain or from another HRP-bound MB^+ molecule or *via* a collisional

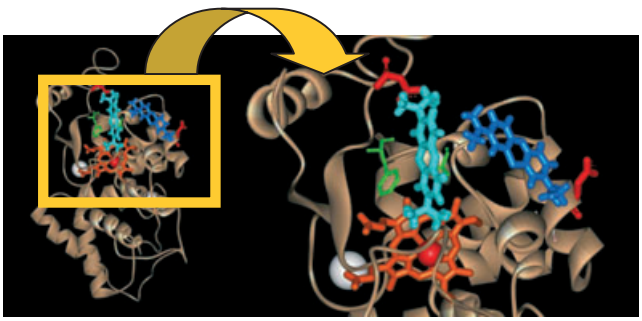

Figure 6. Cartoon showing possible sites for MB^+ binding on HRP structure. Left panel—MB-bound HRP structure. Except when indicated, the amino acid lateral side chains are not shown for clarity. Right panel corresponds to a zoom of the heme crevice. The models were generated by using ArgusLab docking software (20).

mechanism. According to the molecular model, the photoconversion of MB^+ (light blue dye molecule) to $MB^\bullet$ eliminates the electrostatic interaction of the dye with a negatively charged amino acid, here represented by Asp182 (red side chain), decreasing the affinity to the enzyme. In this condition, the binding could result from the remaining hydrophobic interaction between the dye molecule and amino acid residues such as Phe and Pro (green amino acid side chain). In this regard, the docking performed by using the neutral form of the dye showed affinity for the same HRP region (data not shown).

According to the results presented above the following mechanisms could be proposed for the HRP catalytic cycle triggered by hydrogen peroxide in the dark and/or in the absence of MB^+ and under irradiation in the presence of MB^+ (Schemes 2 and 3, respectively).

In the dark and/or in the absence of MB^+, the addition of hydrogen peroxide in an HRP-containing medium triggers the well-known peroxidase cycle. The catalytic cycle observed when hydrogen peroxide was the only available substrate could implicate that peroxide acts as both oxidizing (formation of compound I) and reducing agents (formation of compound II and regeneration of native form) of the heme iron. Peroxidases have been found to utilize HOOH to reduce compound I when no other substrate is available (25,26). In this case, one electron reduction of compound I by HOOH generates $O_2^{-\cdot}$ and compound II, which reacts with another HOOH molecule producing H_2O and compound III (oxyperoxidase). The reaction of compound II with hydrogen peroxide is proposed to occur *via* two paths: in path 1, the reaction of ferryl peroxidase with hydrogen peroxide is preceded by dissociation of the hydroxyl anion and in path 2, hydrogen peroxide is oxidized by ferryl peroxidase to a superoxide radical, which reacts with ferric peroxidase to form compound III. Anyway, compound III quickly decays to the native form and generates ion superoxide. Compound III formation results in enzyme turnover in the absence of reducing substrates; however, progressive irreversible enzyme inactivation has been also identified under this condition probably due to the attack of ion superoxide to enzyme structure (13).

The addition of MB^+ in an HRP-containing medium led to the formation of a complex protein dye in which, under illumination, MB^+ binding could occur before or after the photoreduction. The addition of hydrogen peroxide converts free and dye-bound HRP in the high valence form compound I. Considering that MB^+ could occupy the heme crevice (Fig. 6), the irradiation of the dye could generate $MB^\bullet$ in the proximity of heme iron. In this condition, $MB^\bullet$ is expected to act as the principal photo-reducer agent of the HRP high valence intermediates produced by the addition of hydrogen peroxide. Thus, in samples illuminated in the presence of MB^+ the HRP catalytic cycle is considerably accelerated.

The capacity of $MB^\bullet$ to act as reducing agent for HRP high valence intermediates raises the possibility that the photochemical interference of MB^+ in the PO oscillator could not be restricted to the oxidation of NADPH (15). In the PO oscillator, a catalytic cycle is initiated when NADPH reduces native ferric HRP to the ferrous form and it is converted to $NADP^\bullet$. The Fe^{2+} HRP reacts with O_2 to form compound III that is oxidized by $NADP^\bullet$ to compound I. The cycle is completed by the consecutive reduction of compounds I and II by NADPH. Although the PO cycle is feasible only in the presence of O_2, a condition that lessens the reduction of HRP high valence intermediates by $MB^\bullet$, the findings presented in this work point out the possibility that photogenerated $MB^\bullet$ could, besides NADPH, contribute, even minimally, to the consecutive reduction of compound I and compound II.

CONCLUSIONS

Methylene blue is able to bind in HRP structure and forms the neutral radical $MB^\bullet$ in a feature that allows electron transfer to the high valence forms of the enzyme. The UV–visible spectrum of the HRP-bound MB^+ does not suggest the formation of stacked dimers of the dye. The binding of MB^+ in the HRP structure led to changes in the MB^+ triplet spectrum obtained by the flash photolysis technique.

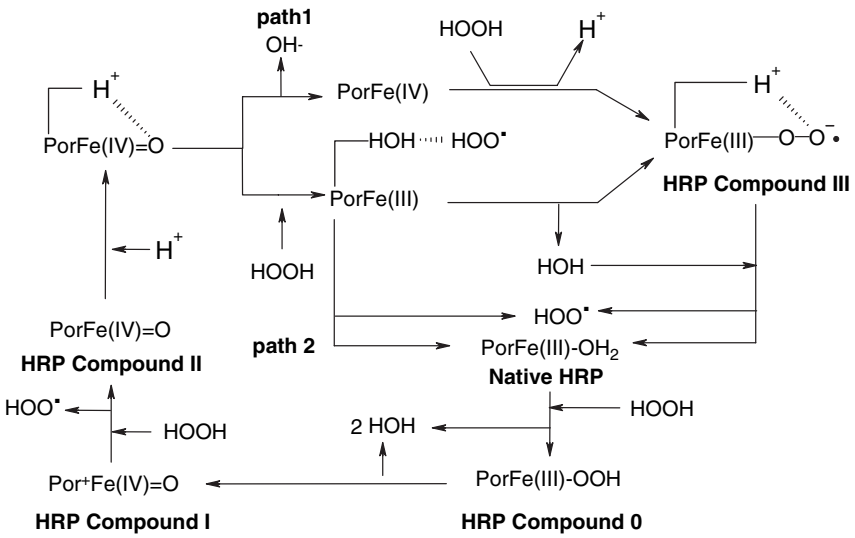

Scheme 2. HRP catalytic cycle by using HOOH as both oxidizing and reducing agents.

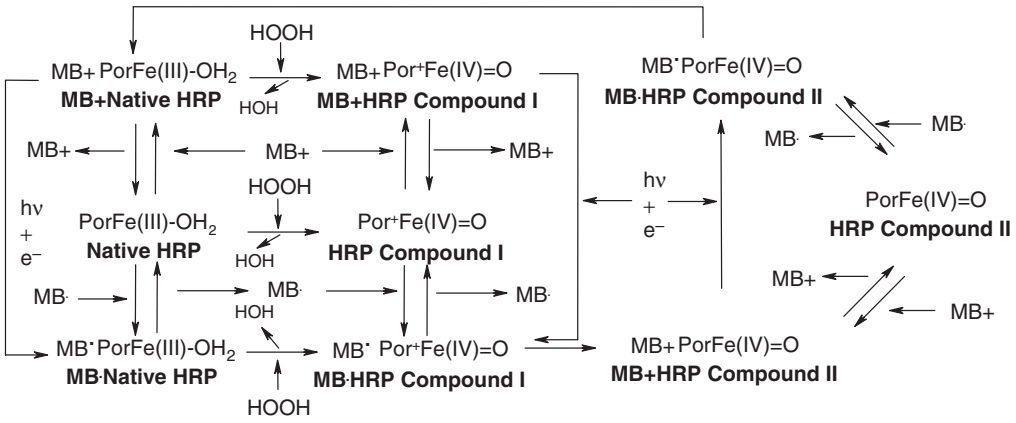

Scheme 3. HRP catalytic cycle by using HOOH as oxidizing agent and $MB^{\bullet}$ as reducing agent.

The neutral radical ($MB^{\bullet}$) generated from the excited state of MB^{+} can promote the reduction of the high valence intermediates of HRP, compounds I and II and accelerate the completion of the enzyme cycle. The kinetic data obtained in air- and argon-saturated medium reveal that MB^{+}, the steady-state predominant form in the presence of molecular oxygen, exhibits 10-fold higher affinity to the HRP heme crevice than $MB^{\bullet}$, but its inability to reduce the heme iron decreases significantly the maximal rate. In the presence and in the absence of oxygen, the curve for the rate of the reaction as a function of MB^{+} concentration exhibited saturation in accordance with MB^{+} binding on the HRP structure. We considered two possible mechanisms for the photogeneration of $MB^{\bullet}$ in the presence of HRP: (1) the binding of two MB^{+} molecules on a HRP molecule allows that, under excitation, triplet MB^{+} can abstract one electron from another dye molecule in the ground state to form $MB^{\bullet}$ that is able to reduce HRP compounds I and II; (2) monomeric $MB^{\bullet}$ generated by electron abstraction of an amino acid residue of the protein was responsible for enzyme reduction.

The participation of photo-generated $MB^{\bullet}$ as the reducing agent in the HRP cycle is evident by the following findings: (1) changes in the pH curve for the reduction of compound II in the presence of photoactivated MB^{+}; (2) matching of the pK_a values obtained from the pH curve of HRP compound II reduction by photoactivated MB^{+} and from the pH curve of triplet MB^{+} reactivity; (3) decrease in the $MB^{\bullet}$ lifetime in the presence of HRP compound II but not in the presence of native HRP; (4) decrease in the lifetime of the HRP oxoferryl species in the presence of photoactivated MB^{+}.

EPR measurements obtained during the reaction of HRP with hydrogen peroxide in the absence and in the presence of irradiated MB^{+} show the formation of $g = 1.998$ species that could be assigned to the HRP oxoferryl π cation (compound I, spin 1/2) (24).

For the first time a light-driven HRP cycle is described. The use of light to activate the reducing agent introduces a turn on/off device in the cycle control. Therefore, this finding could be useful in making use of solar energy in several fields of nanotechnology.

Acknowledgements—The authors thank Fundação de Amparo à Pesquisa do Estado de São Paulo (FAPESP, Pronex—Projeto Temático 2003/09859-2), Conselho Nacional de Pesquisa (CNPq: Proc. 476119/2004-9 and CT-FVA/CNPq 01/2003 Proc. 400618/2004-4) and Fundação de Amparo ao Ensino e Pesquisa da Universidade de Mogi das Cruzes (FAEP-UMC) for financial support. V.A.S. is a fellow of CNPq and H.C.J. is a fellow of FAPESP.

REFERENCES

1. Veitch, N. C. (2004) Horseradish peroxidase: A modern view of a classic enzyme. *Phytochemistry* **65**, 249–259.
2. Welinder, K. G. (1976) Covalent structure of glycoprotein horseradish peroxidase. *FEBS Lett*. **72**, 19–23.
3. Yang, B. Y., J. S. S. Gray and R. Montgomery (1996) The glycans of horseradish peroxidase. *Carbohydr. Res*. **287**, 203–212.
4. Veitch, N. C. and A. T. Smith (2001) Horseradish peroxidase. *Adv. Inorg. Chem*. **51**, 107–162.
5. Dunford, H. B. (1991) Horseradish peroxidase: Structure and kinetic properties. In *Peroxidases in Chemistry and Biology*, **Vol. 2** (Edited by K. E. Everse and M. B. Grisham), pp. 1–24. CRC Press, Boca Raton, FL.
6. Dunford, H. B. (1999) *Heme peroxidases*. Wiley-VCH, New York.
7. Spadaro, J. T. and V. Renganathan (1994) Peroxidase-catalyzed oxidation of azo dyes: Mechanism of disperse yellow 3 degradation. *Biochem. Biophys*. **312**, 301–307.
8. Heinfling, A., M. J. Martínez, A. T. Martínez, M. Bergbauer and U. Szewzyr (1998) Transformation of industrial dyes by manganese peroxidases from *Bjerkandera adusta* and *Pleurotus eryngii* in a manganese-independent reaction. *Appl. Environ. Microbiol*. **64**, 2788–2793.
9. Ollikka, P., K. Alhonmäki, V. M. Leppänen, T. R. Glumoff and I. Suominen (1993) Decolorization of azo, triphenyl methane, heterocyclic, and polymeric dyes by lignin peroxidase isoenzymes from *Phanerochaete chysosporium*. *Appl. Environ. Microbiol*. **59**, 4010–4016.
10. Tuiete, E. M. and J. M. Kelly (1993) Photochemical interactions of methylene blue and analogues with DNA and other biological substrates. *J. Photochem. Photobiol*. **21**, 103–124.
11. Severino, D., H. Junqueira, D. Gabriele, M. Gugliotti and M. S. Baptista (2003) Influence of negatively charged interfaces on the ground and excited state properties of methylene blue. *Photochem. Photobiol*. **77**, 459–468.
12. Estevam, M. L., O. R. Nascimento, M. S. Baptista, P. D. Mascio, F. M. Prado, A. F. Alario, M. R. Zucchi and I. L. Nantes (2004) Changes in the spin state and reactivity of cytochrome *c* induced by photochemically generated singlet oxygen and free radicals. *J. Biol. Chem*. **279**, 39214–39222.

13. Han, S., M. Zhu, Z. Yuan and X. Li (2000) A methylene blue-mediated enzyme electrode for the determination of trace mercury (II), mercury (I), methylmercury, and mercury-glutathione complex. *Biosens. Bioelectron.* **16**, 9–16.
14. Hauser, M. J. B., A. Lunding and L. F. Olsen (2000) On the role of methylene blue in the oscillating peroxidase-oxidase reaction. *Phys. Chem. Chem. Phys.* **2**, 1685–1692.
15. Carson, J. J. L. and J. Walleczek (2003) Response of the peroxidase-oxidase oscillator to light is controlled by MB^{+}-NADH photochemistry. *J. Phys. Chem. B* **107**, 8637–8642.
16. Hauser, M. J. B. and L. F. Olsen (1996) Experimental studies of the mechanism of the peroxidase-oxidase reaction. In *Plant Peroxidases: Biochemistry and Physiology IV: International Symposium of Plant Peroxidases* (Edited by C. Obinger, U. Burner, R. Ebermann, C. Penel and H. Greppin), pp. 82–88. Université de Geneve, Geneva, Vienna.
17. Hauser, M. J. B. and L. F. Olsen (1998) The role of naturally-occurring phenols in inducing oscillations in the peroxidase-oxidase reaction. *Biochemistry* **37**, 2458–2469.
18. Møller, A. C., M. J. B. Hauser and L. F. Olsen (1998) Oscillations in peroxidase-catalyzed reactions and their potential function in vivo. *Biophys. Chem.* **72**, 63–72.
19. Nelson, D. P. and L. A. Kiesow (1972) Mechanism of reaction of myeloperoxidase with hydrogen peroxide and chloride ion. *Anal. Biochem.* **49**, 474–478.
20. Thompson, M. A. *ArgusLab 4.0.1*. Planaria Software LLC, Seattle, WA, http://www.arguslab.com. Accessed on 25 May 2007.
21. Baptista, M. S. and G. L. Indig (1998) Effect of BSA binding on photophysical and photochemical properties of triarylmethane dyes. *J. Phys. Chem. B* **102**, 4678–4688.
22. Nakagima, R. and I. Yamazaki (1987) The mechanism of oxyperoxidase formation from ferryl peroxidase and hydrogen peroxide. *J. Biol. Chem.* **262**, 2576–2581.
23. Junqueira, H. C., D. Severino, L. G. Dias, M. Gugliotti and M. S. Baptista (2002) Modulation of methylene blue photochemical properties base don adsorption at aqueous micelle interfaces. *Phys. Chem. Chem. Phys.* **4**, 2320–2328.
24. Schulz, C. E., R. Rutter, J. T. Sage, P. G. Debrunner and L. P. Hager (1984) Mossbauer and electron paramagnetic resonance studies of horseradish peroxidase and its catalytic intermediates. *Biochemistry* **23**, 4743–4754.
25. Claiborne, A. and I. Fridovich (1979) Purification of the o-dianisidine peroxidase from *Escherichia coli* B. Physicochemical characterization and analysis of its dual catalatic and peroxidatic activities. *J. Biol. Chem.* **254**, 4245–4252.
26. Hiner, A. N. P., J. H. Ruiz, J. N. R. López, F. G. Cánovas, N. C. Brisset, A. T. Smith, M. B. Arnao and M. Acosta (2002) Reactions of the class II peroxidases, lignin peroxidase and *Arthromyces ramosus* peroxidase, with hydrogen peroxide. *J. Biol. Chem.* **277**, 26879–26885.